Int. J. of Thermodynamics
ISSN 1301-9724
Vol. 13 (No. 4), pp. 153-160, 2010
www.icatweb.org/ijot

An Analysis of Unglazed Transpired Solar Collectors Based on Exergetic Performance Criteria

Sadegh Motahar*, Ali Akbar Alemrajabi

Department of Mechanical Engineering, Isfahan University of Technology, Isfahan 84156, I.R.Iran
E-mail: smotahar@me.iut.ac.ir

Abstract

In this paper, an exergetic performance analysis of unglazed transpired collectors (UTC), as well as an exergetic optimization of a typical UTC is performed. A steady-state model is used to calculate heat transfers and pressure drop through the perforated plate and back wall. In order to maximize the exergy efficiency, the optimization procedure is carried out for some important parameters including plate hole diameter and hole pitch. A maximum efficieny of 2.28% is obtained. In spite of all the thermal performance advantages, the exergetic efficiency of the UTC is significantly lower than its energetic efficiency. Other parameters such as incident solar radiation, approach velocity, plate hole diameter and pitch are examined in the parametric study.

Keywords: *Unglazed transpired collector; exergetic performance; optimization.*

1. Introduction

An unglazed transpired collector (UTC) is a renewable energy technology that is well proven and has a considerable potential for commercial and industrial applications (Hollick, 1994). By preheating ventilation air with solar energy, the technology removes a substantial load from a building's conventional heating system, saving energy and money (Hollick, 1994). In addition to solar ventilation air preheating systems, other applications such as sun drying in agricultural sector (Hollick, 1999), desiccant cooling (Pesaran and Wipke, 1994), and paring photovoltaic with UTC (PV/Thermal systems) are generally developed.

Many research papers were involved in UTC modeling as well as in the practical development of such systems. Kutscher, Christensen & Barker (1993) presented a review of the heat loss theory applied to the UTC by providing a simple heat balance on collector. Kutscher (1994) performed some experiments on a small test collector to determine the heat exchange effectiveness as well as to predict pressure drop for the collector and noted that important parameters included air flow rate, crosswind speed, hole pitch, and hole diameter. Van Decker, Hollands & Brunger (2001) investigated the heat exchange effectiveness more thoroughly for three-dimensional flow. Fleck, Meier & Matovic (2002) addressed wind effects through a field study on a UTC. A mathematical model for a UTC is performed to predict the thermal performance of UTC over a wide range of design and operating conditions by Augustus Leon & Kumar (2007). They varied the porosity, airflow rate, solar radiation, and solar absorptivity and thermal emissivity, and found their influence on collector efficiency, heat exchange effectiveness, air temperature rise and useful heat delivered. Their results indicate promising thermal performance for a UTC, offering itself as an attractive alternate to glazed solar collectors for drying of food products.

Exergy analysis is a thermodynamic analysis technique based on the second law of thermodynamics, which provides an alternative means of assessing and comparing solar systems. In particular, exergy analysis yields efficiencies which provide a true measure of how nearly actual performance approaches the ideal, and identifies more clearly than energy analysis the causes and locations of thermodynamic losses. Consequently, exergy analysis can assist in improving and optimizing solar air heating (SAH) system designs. In this matter, Torres-Reyes & Navarrete-Gonzalez (2002), Luminosu & Fara (2005), Gupta & Kaushik (2008) and Farahat, Sarhaddi & Ajam (2009) have investigated exergy analysis and exergetic optimization of SAH systems. However, an exergy-based performance analysis has not been considered for UTCs previously and a study is required to investigate exergetic performance for such SAH systems.

In the present study, an exergetic performance analysis of unglazed transpired solar collectors utilized in preheating ventilation air has been accomplished. A simulation program, including heat transfer equations, energy and exergy balances, has been developed in MATLAB. Exergy efficiency as an objective function has been maximized subjected to UTC perforation parameters, namely hole pitch and hole diameter. In addition, variations of exergetic performance are evaluated in terms of UTC design parameters and operating conditions.

2. UTC Governing Equations

2.1 General Considerations

UTCs consist of a perforated, solar-absorbing plate mounted on a large south-facing wall (Hollick, 1994). Air is drawn into the plenum through the holes in the plate, up the plenum, and finally into the building, as shown in Figure 1.

UTC system saves energy in three ways (Summers, 1995): 1) solar energy absorption by the collector and convection to the air as it flows through the collector; 2) heating the plenum air by energy convected from the outside wall surface; and, 3) reduction in conduction through the wall due to the low temperature difference across the outside wall.

*Corresponding Author

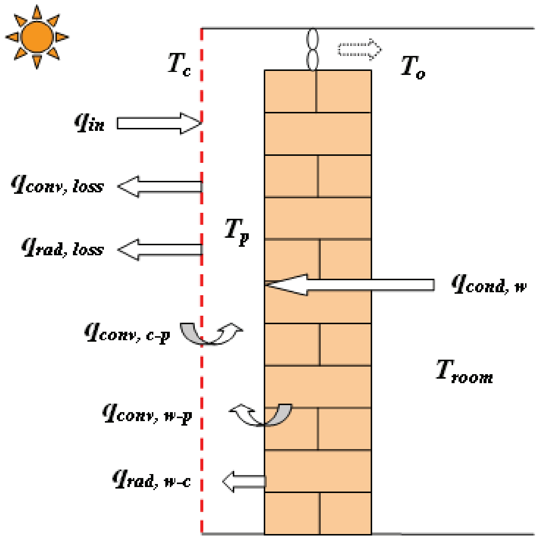

Figure 1. Heat transfer modes in UTC.

The following assumptions are considered in UTC modeling:

- The air in the plenum only flows vertically, not horizontally, and the UTC system becomes two-dimensional.
- The air temperature in the plenum and collector plate temperature are assumed to be uniform
- The collector plate has holes oriented on a triangular pitch.

2.2 Energy Analysis

The heat transfer modes are illustrated in Figure 1 in order to predict the thermal performance of UTC. The energy balance equations for the solar-absorbing plate and the back wall can be written as:

$$q_{in} + q_{rad,w-c} = q_{conv,c-p} + q_{conv,loss} + q_{rad,loss} \tag{1}$$

$$q_{cond,w} = q_{conv,w-p} + q_{rad,w-c} \tag{2}$$

The labeling convention for heat flows is $q_{\text{mode, from-to}}$ .The absorbed energy by the perforated plate is:

$$q_{in} = \alpha_c I_T A_s \tag{3}$$

where $A_s = (1-\sigma)A$, is the collector surface area, i.e. the total frontal area (A) minus the hole area. The plate porosity, σ , can be expressed as (Kutscher ,1994):

$$\sigma = 0.907(D/P)^2 \tag{4}$$

The radiant exchange between the back wall outer surface and collector plate is:

$$q_{rad,w-c} = \sigma_{sb} A(T_w^4 - T_c^4)/(1/\varepsilon_w + 1/\varepsilon_c - 1) \tag{5}$$

where the denominator is the view factor between the collector plate and back wall (Incropera, DeWitt, Bergman & Lavine, 2007).

The air flowing through the collector into the plenum convects energy from the collector surface (Augustus Leon & Kumar, 2007) and (Summers, 1995).

$$q_{conv,c-p} = \dot{m}_c C_p (T_p - T_a) = \dot{m}_c C_p \varepsilon_{HX} (T_c - T_a) \tag{6}$$

with $\dot{m}_c = \rho V_s A$. The heat exchange effectiveness can be written as follows (Kutscher ,1994):

$$\varepsilon_{HX} = \frac{T_o - T_a}{T_c - T_a} = 1 - \exp\left(-\frac{kNu_D(1-\sigma)}{D\rho V_s C_p}\right) \tag{7}$$

For $0.1\% < \sigma < 5\%$ and $100 < \mathrm{Re}_D < 2000$, the following correlation for Nusselt number predicts heat exchange effectiveness (Kutscher, 1994):

$$Nu_D = 2.75\left[\left(\frac{P}{D}\right)^{-1.2} \mathrm{Re}_D^{0.43} + 0.011\sigma \,\mathrm{Re}_D \left(\frac{U_\infty}{V_s}\right)^{0.48}\right] \tag{8}$$

where $\mathrm{Re}_D = V_h D/\nu$ is the hole's Reynolds number with a hole velocity of $V_h = V_s/\sigma$.

For corrugated transpired solar collectors, convective losses to the surrounding must not be neglected and can be written as:

$$\begin{aligned} q_{conv,loss} &= \frac{Nu_{loss} k}{H} A(T_c - T_a) \\ Nu_{loss} &= 0.82 \frac{\rho C_p U_\infty \nu}{k V_s} C_f \end{aligned} \tag{9}$$

The radiative losses to the surrounding are calculated by:

$$\begin{aligned} q_{rad.loss} &= \varepsilon_c \sigma_{sb} A_s (T_c^4 - T_{sur}^4) \\ T_{sur}^4 &= 0.5(T_{sky}^4 + T_{gr}^4) \\ T_{sky} &= 0.0552 T_a^{1.5}, T_{gr} \cong T_a \end{aligned} \tag{10}$$

The outside surface of the wall gains energy by conduction through the wall from the inside room (Summers, 1995):

$$q_{cond,w} = U_{cond,w} A(T_{room} - T_w) \tag{11}$$

The convective heat transfer from outer wall to plenum air is (Incropera et al, 2007):

$$\begin{aligned} q_{conv,w-p} &= \frac{kNu_H}{H} A(T_w - T_p) = \dot{m}_c C_p (T_o - T_p) \\ Nu_H &= \begin{cases} 0.664\,\mathrm{Re}_H^{0.5}\,\mathrm{Pr}^{0.333} & \mathrm{Re}_H < 5\times 10^5 \\ \left(0.037\,\mathrm{Re}_H^{0.8} - 871\right)\mathrm{Pr}^{0.333} & \mathrm{Re}_H > 5\times 10^5 \end{cases} \end{aligned} \tag{12}$$

The energy balances, Eqs. (1)-(2), are solved in MATLAB. These equations reduce to two unknowns, the wall temperature and the collector temperature. The useful energy or the heat delivered to the building is determined by:

$$q_u = \dot{m}_c C_p (T_o - T_a) \tag{13}$$

and finally, the thermal efficiency ($\eta = q_u / I_T A$) of the collectors can be evaluated.

2.3 Pressure Drop Calculation Through Collector and Plenum

Required power is related to the total pressure drop in the system that must be overcome by the fan including the pressure drop across the face of the collector, the friction in the plenum, the buoyancy force of the air, and the acceleration of the air in the system:

$$\Delta P_{tot} = \Delta P_c + \Delta P_{fric} + \Delta P_{bouy} + \Delta P_{acc} \tag{14}$$

The following equations are used to calculate the pressure drop across the UTC:

$$\Delta P_c = \frac{1}{2}\rho V_s \zeta \qquad \zeta = 6.82\left(\frac{1-\sigma}{\sigma}\right)\mathrm{Re}_D^{-0.236} \tag{15}$$

$$\Delta P_{fric} = f\,\frac{H\rho V_p^2}{2D_h} \qquad V_p = \frac{1}{2}\frac{V_s H}{D_p},\ D_h = \frac{4(D_p \times W)}{2(D_p + W)} \tag{16}$$

$$\Delta P_{bouy} = \frac{1}{2}(\rho_o - \rho_a) g H \tag{17}$$

$$\Delta P_{acc} = \frac{1}{2}\rho (2V_p)^2 \tag{18}$$

The total fan power required can be calculated from:

$$\dot{W}_{fan} = \frac{\dot{m}_c \Delta P_{tot}}{\rho} \tag{19}$$

2.4 Exergy Analysis

Exergy is the maximum amount of work that can be extracted from a system (Dincer & Rosen, 2007). For real processes the exergy input always exceeds the exergy output, and this unbalance is due to irreversibilities. The irreversibility is calculated by setting up the exergy balance and taken the difference between all incoming and outgoing exergy flows.

The exergy flows in the UTC are illustrated in Figure 2. An exergy balance for the UTC can be written as:

$$\dot{E}x_{solar} + \dot{E}x_w + [\dot{E}x_{q_{cond}}]^+ + \dot{E}x_{in} = \dot{E}x_{q_{loss}} - [\dot{E}x_{q_{cond}}]^- + \dot{E}x_{out} + \dot{I} \tag{20}$$

where the meaning of the + (or similarly -) exponent is that only positive (negative) values of the term in the square bracket are to be used (i.e. use zero if the term is negative (positive)). When the room temperature is greater than the back wall temperature, $\dot{E}x_{q_{cond}} > 0$; otherwise $\dot{E}x_{q_{cond}} < 0$.

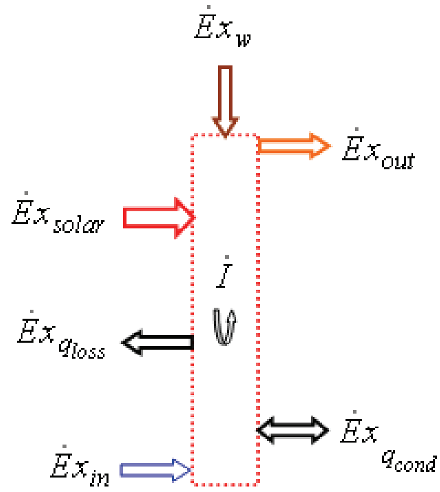

Figure 2. Exergy flows in UTC.

The exergy of solar radiation can be expressed, by modifying the expression of Petela (Dincer & Rosen, 2007) as follows:

$$\dot{E}x_{solar} = I_T A_s \left(1 - \frac{4T_a}{3T_S} + \frac{1}{3}\left(\frac{T_a}{T_S}\right)^4\right) \tag{21}$$

where T_S is the sun's surface temperature, taken to be 6000 K. The following relations are available for other components:

$$\dot{E}x_w = \dot{W}_{fan} \tag{22}$$

$$\dot{E}x_i = \dot{m}_c\left[(h_i - h_a) - T_a(s_i - s_a)\right] \tag{23}$$

$$\dot{E}x_{q_{loss}} = (q_{conv,loss} + q_{rad,loss})\left(1 - \frac{T_a}{T_c}\right) \tag{24}$$

$$\dot{E}x_{q_{cond}} = q_{cond}\left(1 - \frac{T_a}{T_w}\right) \tag{25}$$

where $\dot{E}x_i$ is the exergy associated with the mass flow of air entering or leaving the control volume. According to Figure 2, if heat conducts from the room to the plenum (positive sign for $\dot{E}x_{q_{cond}}$ in Eq. (20)), it can boost the used exergy, but in the reverse case, this process results in exergy loss via conduction (negative sign for $\dot{E}x_{q_{cond}}$ in Eq. (20)).

The used exergy, $\dot{E}x_{used}$, is the required exergy input for the process to be performed.

$$\dot{E}x_{used} = \dot{E}x_{solar} + \dot{E}x_w + [\dot{E}x_{q_{cond}}]^+ \tag{26}$$

Table 1. Properties of air.

	A	B	C	D	E
C_P (J/kgK)	1.933E-10	-7.999E-07	1.141E-03	-4.489E-01	1.058E+03
ν (m^2/s)	0	-1.156E-14	9.573E-11	3.760E-08	-3.448E-06
k (W/mK)	0	1.521E-11	-4.857E-08	1.018E-04	-3.933E-04
α (m^2/s)	0	0	9.102E-11	8.820E-08	-1.065E-05

The desired output exergy, $\dot{E}x_{desired}$ (or the useful exergy gain, $\dot{E}_u$) is calculated by:

$$\dot{E}x_{desired} = \dot{E}x_{out} - \dot{E}x_{in} \tag{27}$$

The exergy efficiency of UTC, i.e. the ratio of desired exergy to used exergy, is determined from Eq. (28):

$$\psi = 1 - \frac{\dot{E}x_{q_{loss}} - [\dot{E}x_{q_{cond}}]^{-} + \dot{I}}{\dot{E}x_{solar} + \dot{E}x_{w} + [\dot{E}x_{q_{cond}}]^{+}} \tag{28}$$

The meaning of the + and - exponents is mentioned above.

3. Air Properties

The thermophysical properties of air are calculated from polynomial curve fits to a data set in Incropera et al (2007) for convenience in programming. They can be written in the form of $AT^4 + BT^3 + CT^2 + DT + E$ with their constants are found in Table 1. Also the air density can be obtained from $\rho = 360.7782T^{-1.00336}$ (kg/m^3).

4. Validation of the UTC Model

Experiments on UTC performance have been done at the National Solar Test Facility (NSTF), Canada (Summers, 1995). Hollick (1994) presented curve fits of the data. These curve fits of air temperature rise ($T_p - T_a$) as a function of solar radiation are plotted in Figure 3 for three flow rates (130, 72 and 36 m/h). The UTC plates used in these experiments have the parameters in Table 2 (Summers, 1995). The room temperature is set to 22°C. The NSTF experiments were performed indoors at room temperature. Results based on the model developed in Section 2 are shown as compared to experimental results in Figure 3.

At an approach velocity of 130 m/h the model slightly under predicts the air temperature rise at high solar radiation. For an approach velocity of 72 m/h the UTC model agrees with the empirical results at intermediate solar radiation. At lower approach velocities, the UTC model substantially over predicts the performance of the collector. Assuming no convection loss is the reason for the over estimation of the UTC performance at low approach velocities.

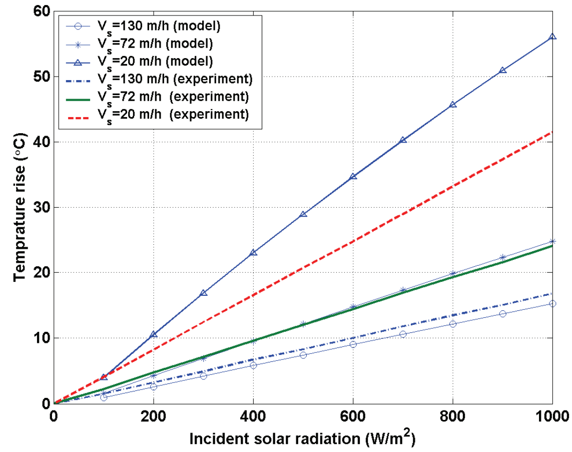

Figure 3. Air temperature rise versus incident solar radiation (figure is in color in the on-line version of the paper).

5. Optimization Procedure

Optimization techniques are used to find a set of design parameters, $\boldsymbol{x}=\{x_1,x_2,\ldots,x_n\}$, that can in some way be defined as optimal. In a simple case this might be the minimization or maximization of some system characteristic that is dependent on $\boldsymbol{x}$. In this paper, the optimization problem is initially stated as follows:

Maximize $f(\boldsymbol{x})$,

Subject to:

$h_j(\boldsymbol{x})=0$ $\quad$ $,j=1,2,\ldots,m$

$g_k(\boldsymbol{x})\leq 0$ $\quad$ $,k=1,2,\ldots,p$

$x_i^L \leq x_i \leq x_i^U$ $\quad$ $,i=1,2,\ldots,n$

where x_i^L and x_i^U are the lower and upper limits of x_i. A sequential quadratic programming (SQP) method has been used. The method finds a constrained maximum of a scalar function of several variables starting at an initial estimate. This is generally referred to as constrained nonlinear optimization or nonlinear programming.

The considered objective function is the exergy efficiency of the UTC (Eq. (28)). In a UTC, the hole diameter and the hole pitch are very important design parameters corresponding to the heat transferring performance and pressure drop within the collector. It is desired to determine the optimum hole size and arrangement of the UTC that maximizes the exergy efficiency, $\psi(P,D)$ subject to the equality constraint functions, i.e. Eq. (1)-(2). The inequalities used as constraint functions are $12 \leq P \leq 24$ and $0.8 \leq D \leq 1.55$

(P and D in mm). Exergy efficiency optimization has been performed using the MATLAB optimization toolbox.

6. Results and Discussions

In the following section, results of the optimization and exergetic performance of the UTC are presented. The numerical calculations are carried out by employing the values of the relevant parameters as follows: $T_a = 10^\circ C$, $T_{room} = 20^\circ C$, $V_s = 0.02\,m/s$, $U_\infty = 1.2\,m/s$, $I_T = 800\,W/m^2$, $\varepsilon_w = 1$, $(UA)_W = 1$, $C_f = 1$, and the parameters in Table 2. When one parameter is varied, the others are kept constant.

Table 2. The UTC parameters.

parameter	value
Collector height (m)	2.44
Collector length (m)	1.83
Plenum depth (m)	0.0762
Hole diameter (m)	0.00159
Hole pitch (m)	0.0214
Absorptivity of collector	0.90
Emissivity of collector	0.90

6.1 Optimum Hole Diameter and Hole Pitch

The optimization procedure is run and optimum hole diameter and pitch are found as $D = 0.9mm$ and $P = 12mm$. The maximum exergy efficiency with respect to these conditions will be $\psi = 2.28\%$. Inserting the above results in the constraints, the other UTC operating parameters are determined as follows: $T_p = 30.63^\circ C$, $T_w = 35.55^\circ C$, $T_c = 37.15^\circ C$, $T_o = 30.9^\circ C$, $\eta = 65.65\%$, $\dot{I} = 3392.3W$, $E_u = 80.87W$, $\sigma = 0.5\%$, $\varepsilon_{HX} = 75.99\%$, $A_s = 4.44m^2$, and $\dot{m}_c = 0.111kg/s$.

The exergetic optimization of this system shows that it should be modified based on the above perforation parameters to deliver maximum exergetic efficiency, although this efficiency is very low. Design of such a modified system is feasible based on the above UTC optimization parameters.

Figure 4 indicates the exergy efficiency contours according to the hole diameter and hole pitch in two dimensions. The exergy efficiency is sensitive to hole diameter and hole pitch.

6.2. Effect of Incident Solar Radiation on Exergetic Performance

Figure 5 shows the variation of desired exergy and irreversibility of the UTC with incident solar radiation on the UTC. Because of the growth in the exergy received by the collector with incident solar radiation, the UTC useful exergy increases with incident solar radiation as well as the irreversibility increases.

Figure 6 presents the increase of exergy efficiency of UTC with incident solar radiation on UTC. The exergy efficiency rises notably due to an increase in the UTC useful exergy.

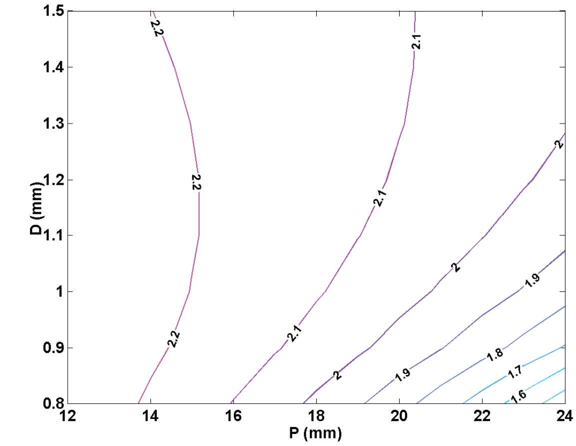

Figure 4. Exergy efficiency contours in various hole diameter and hole pitch.

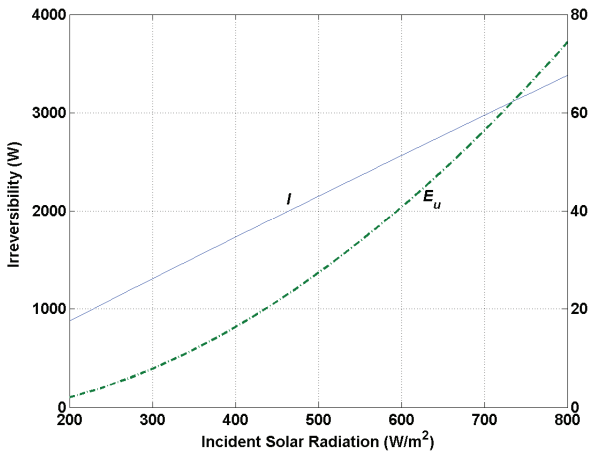

Figure 5. Variation of desired exergy and UTC irreversibility with incident solar radiation.

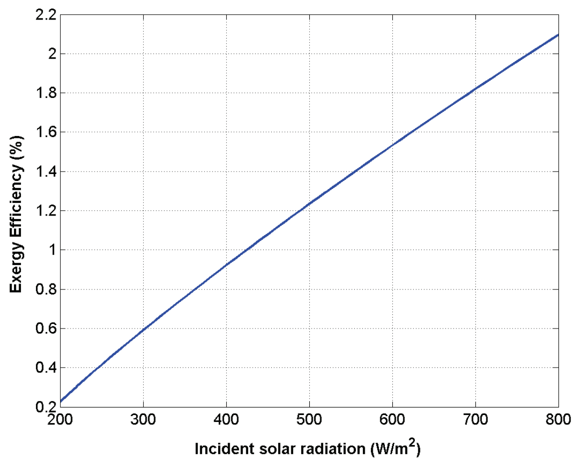

Figure 6. Variation of exergy efficiency with incident solar radiation.

6.3. Effect of Perforation on Exergetic Performance

Perforation depends on two parameters: the plate hole diameter and hole pitch. In Section 6.1, the optimized hole diameter and hole pitch was evaluated. The UTC irreversibility and desired exergy with varying *D* are shown in Figure 7 while all other parameters are held constant. It shows the desired exergy improves from 61.42W to 74.34W when the hole diameter increases from 0.8 mm to 1.6 mm, namely a 21% increase. Contrarily, a decrease of 1.5% in the UTC irreversibility is presented. The growth in the UTC desired exergy is more than the reduction in its irreversibility. Consequently as shown in Figure 8, the exergy efficiency will increase from 1.72% to 2.10% although the thermal efficiency will decrease with hole diameter (Augustus Leon & Kumar, 2007).

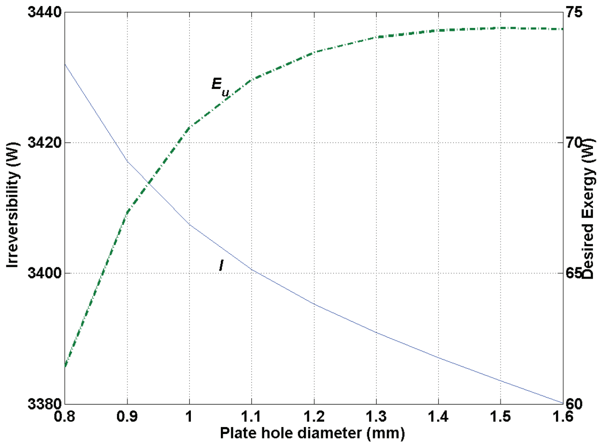

Figure 7. Variation of desired exergy and UTC irreversibility with plate hole diameter.

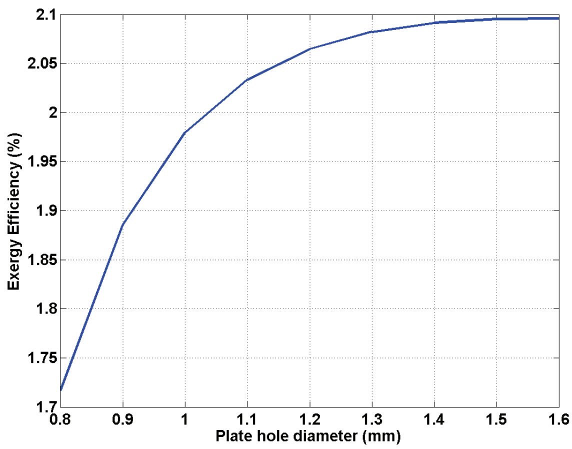

Figure 8. Variation of exergy efficiency with plate hole diameter.

Figure 9 shows the variation of desired exergy and irreversibility of the UTC against plate hole pitch. The UTC irreversibility increases with hole pitch although the desired exergy decreases with hole pitch . In addition, this pattern is seen in Figure 10 for the exergy efficiency versus hole pitch. The thermal efficiency of the UTC decreases continually with hole pitch (Augustus Leon & Kumar, 2007).

Plate hole diameter and hole pitch are collected together in the porosity of the perforated plate. Figure11 illustrates the effect of porosity on exergy efficiency of the UTC. At lower porosities, the plate has a high hole pitch in order to maximize the exergy efficiency. At higher porosities, the plate pitch will reduce and exergy efficiency will decrease with porosity. For constant pitch, increasing the porosity decreases the exergy efficiency.

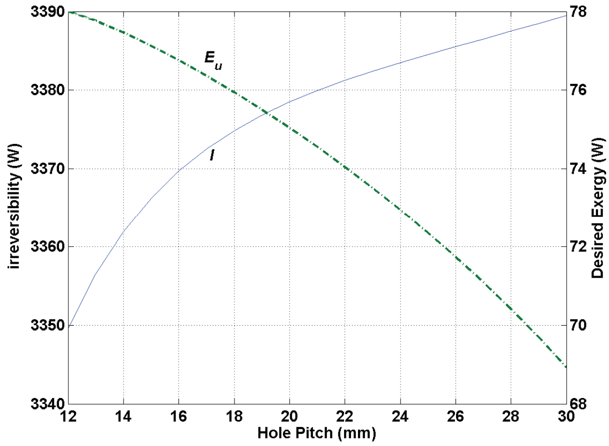

Figure 9. Variation of desired exergy and UTC irreversibility with hole pitch.

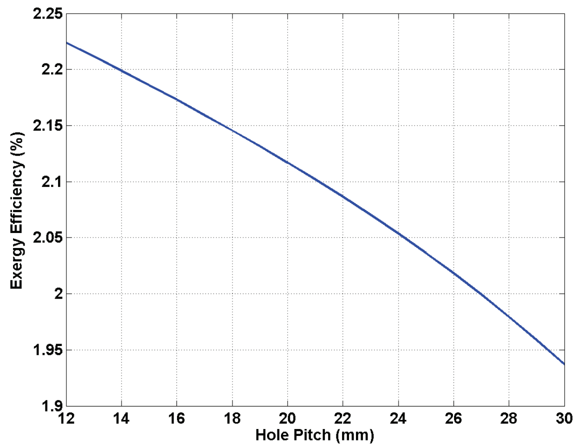

Figure 10. Variation of exergy efficiency with hole pitch.

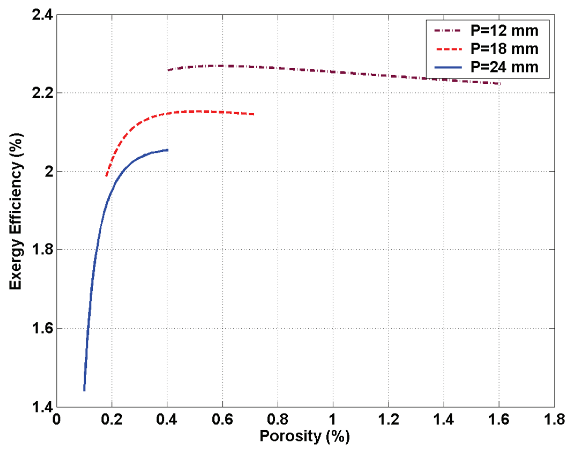

Figure 11. Effect of plate porosity on exergy efficiency.

6.4. Effect of Air Approach Velocity on Exergetic Performance

Figure 12 presents the variation of desired exergy and irreversibility of the UTC with approach velocity. Due to the linear relationship between approach velocity and airflow rate, any increase in approach velocity means a proportional increase in airflow rate. A greater approach velocity across the UTC results in a lower desired exergy and a higher irreversibility. Exergy efficiency therefore decreases at higher approach velocity as shown in Figure 13.

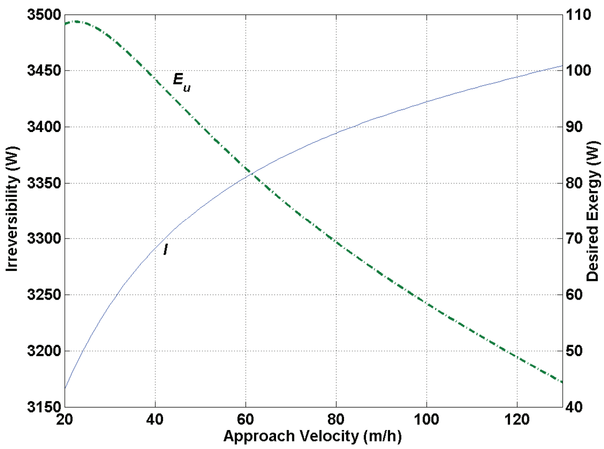

Figure 12. Variation of desired exergy and UTC irreversibility with approach velocity.

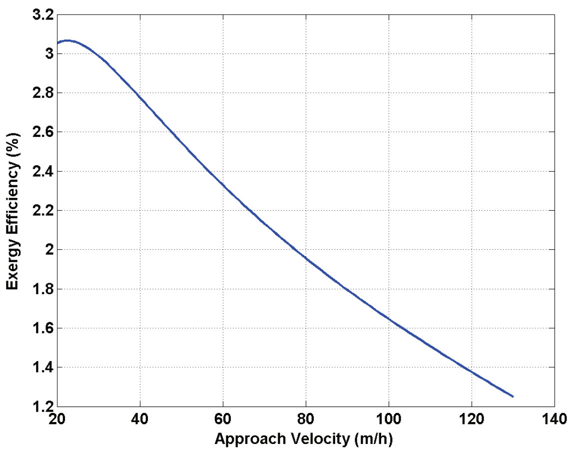

Figure 13. Variation of exergy efficiency with approach velocity.

7. Conclusions

An exergy analysis and optimization of an unglazed transpired collector was performed. The exergetic performance of the UTC based on its energy flows was developed. As an objective function, the exergy efficiency was optimized subject to plate perforation parameters, i.e. the plate hole diameter and pitch, and exergy efficiency contours were illustrated. The exergetic performance of UTC was evaluated using a parametric study which considered some important parameters such as incident solar radiation, hole diameter and pitch of perforated plate and approach velocity over a wide range. Perforation parameters and incident solar radiation had a significant effect on improvement of exergetic performance. Increasing the approach velocity reduced the exergetic performance of the UTC. The exergy analysis indicated that the exergy efficiency of a UTC is notably lower than its thermal efficiency and a comprehensive study should be carried out to improve the second law performance of such a solar system.

Nomenclature

A	total collector area (m^2)
A_s	collector surface area (m^2)
C_f	corrugation factor
C_p	specific heat of air (J/kgK)
D	hole diameter (m)
D_h	plenum hydrolic diameter (m)
D_p	plenum depth (m)
Ex	exergy flow (W)
f	friction factor
g	gravitational constant (9.8066 m/s^2)
H	collector height (m)
$\dot{I}$	irreversibility (W)
I_T	incident solar radiation (W/m^2)
k	thermal conductivity (W/mK)
$\dot{m}$	mass flowrate (kg/s)
Nu	Nusselt number
P	hole pitch (m)
Pr	Prandtl number
ΔP	pressure drop (Pa)
q	heat transfer rate (W)
Re	Reynolds number
T	temperature (K)
U	overall heat transfer coefficient (W/m^2K)
U_∞	wind speed (m/s)
V_h	hole velocity (m/s)
Vs	approach velocity (m/s)
W	collector width (m)
$\dot{W}$	power (W)

Greek symbols

α	absorptivity
α	thermal diffusivity (m^2/s)
ε	emissivity
ε_{HX}	heat exchange effectiveness of collector
η	thermal efficiency
ν	kinematic viscosity (m^2/s)
ρ	air density (kg/m^3)
σ	porosity
σ_{sb}	Stefan Boltzman Constant (5.67×10^{-8} W/m^2K^4)
ψ	exergy efficiency
ζ	dimensionless pressure term

Subscripts

a	ambient
acc	acceleration
$bouy$	buoyancy
c	collector
$cond$	conduction
$conv$	convection
$fric$	friction
gr	ground

in	input
o	outlet
out	output
p	plenum
rad	radiation
S	sun
sur	surrounding
w	wall, work

References

Arulanandam, S. J., Hollands, K. G. T., Brundrett E. (1999). *A CFD heat transfer analysis of the transpired solar collector under no-wind conditions*. Solar Energy, *67*, 93–100.

Augustus Leon, M., Kumar, S. (2007). *Mathematical modeling and thermal performance analysis of unglazed transpired solar collectors*. Solar Energy. *81*, 62-75.

Dincer, I., Rosen, M. A.. (2007). *Exergy: Energy, Environment and Sustainable Development*, (1st ed.). Oxford, Elsevier Science Publishing Company.

Farahat, S., Sarhaddi, F., Ajam H. (2009). *Exergetic optimization of flat plate solar collectors*. Renewable Energy. *34*, 1169-1174.

Fleck, B. A., Meier, R. M., Matovic, M. D. (2002). *A field study of the wind effects on the performance of an unglazed transpired solar collector*. Solar Energy. *73*, 209-216.

Gupta, M. K., Kaushik, S. C. (2008). *Exergetic performance evaluation parametric studies of solar air heater*. Energy. *33*, 1691-1702.

Hollick, J. C. (1994). *Unglazed solar wall air heaters*. Renewable Energy. *5*, 415-421.

Hollick, J. C. (1999). *Commercial scale solar drying*. Renewable Energy. *16*, 714–719.

Incropera, F. P., DeWitt, D. P., Bergman, T. L., Lavine, A. S. (2007). *Fundamentals of Heat and Mass Transfer,* 6th ed.), New York, NY: John Wiley & Sons Inc.

Kutscher, C. F., Christensen, C., Barker, G. (1993). *Unglazed transpired solar collectors: heat loss theory*. Journal of Solar Engineering, *115*, 182–188.

Kutscher, C. F. (1994). *Heat exchanger effectiveness and pressure drop for air flow through perforated plates with and without crosswind*. Journal of Heat Transfer, *116*, 391–399.

Luminosu, I., Fara, L. (2005). *Thermodynamic analysis of an air solar collector*. Int. J. Exergy. *2*, 385-408.

Pesaran, A. A., Wipke, K.. (1994). *Use of unglazed transpired solar collectors for desiccant cooling*. Solar Energy. *52*, 419-427.

Summers, D. N. (1995). *Thermal Simulation and Economic Assessment of Unglazed Transpired Collector Systems*., (M.Sc. Thesis), University of Wisconsin-Madison, USA.

Torres-Reyes, E., Navarrete-Gonzalez, J. J., Ibarra-Salazar, B. A. (2002). *Thermodynamic method for designing dryers operated by flat-plate solar collectors*. Renewable Energy. *26*, 649-660.

Van Decker, G. W. E., Hollands, K. G. T., Brunger, A. P. (2001). *Heat exchange relations for unglazed transpired solar collectors with circular holes on a square or triangular pitch*. Solar Energy. *71*, 33–45.